VOL. 11, NO. 1, JANUARY 2016 ISSN 1819-6608
ARPN Journal of Engineering and Applied Sciences

www.arpnjournals.com

SYNTHESIZATION OF GRAPHENE AND ITS INCORPORATION INTO NATURAL FIBER REINFORCED THERMOSETTING NANOCOMPOSITE

Kim Yeow Tshai[1], Pooria Khalili[1], Ing Kong[1], Chin Hooi Yeoh[1] and Kim Hoe Tshai[2]
[1]The University of Nottingham, Malaysia Campus, Department of Mechanical, Materials and Manufacturing Engineering, Faculty of Engineering, Jalan Broga, Semenyih, Selangor, Malaysia
[2]Faculty of Engineering and Green Technology, Universiti Tunku Abdul Rahman, Jalan Universiti, Bandar Baru Barat, Kampar, Perak, Malaysia
E-Mail: kim-yeow.tshai@nottingham.edu.my

ABSTRACT

Palm EFB epoxy composites were loaded with two variants of graphene of concentration ranging from 0.01 - 0.05*wt*% and the thermal, mechanical and combustibility properties of the nanocomposites were investigated. The graphene considered in this work were a purified graphene derived from exfoliation of expandable graphite and commercially available water-based graphene nanoplatelets UG PRO 680. The results demonstrated that inclusion of a low concentration of graphene capable to yield a composition with improved thermal-mechanical properties and reduces tendency of combustion. However, increasing graphene loading from 0.01 to 0.05*wt*% does not explicitly lead to a more superior performance owing to the greater agglomeration of nanoparticles at high concentration which reduces the effectiveness of homogenous dispersion within the resin matrix.

Keywords: graphene, epoxy, composite, palm fiber, flammability.

INTRODUCTION

Natural fibers are biodegradable and renewable resources that possess several advantages over synthetic fibers such as nonabrasive, low density, good acoustic property, low cost, ease of availability and recyclability [1-2]. In recent years, there has been growing environmental consciousness which raises the interest in utilizing natural fibers as reinforcement in polymer composites [3]. Despite the advantages, processing of natural fiber composites faced several challenges due to their poor wettability, low thermal stability and high moisture absorption properties [4].

Over the last decade, a significant volume of publications in the field of material science has been focused on nanoscale carbon based materials such as carbon nanotubes (CNTs) [5], graphite nanoflakes [6] and graphene oxide sheets [7]. Graphene, a planar monolayer, virtually two dimensional sheets composed of sp^2 carbon atom arranged in a honeycomb lattice with a carbon-carbon bond length of 0.142nm [8] has received intensive attention amongst scientists for their impressive mechanical, thermal, conductivity and lubrication properties. These outstanding performances could be attributed to its tightly packed carbon atoms and the large specific area offered by the crystalline allotrope of carbon aligned in the form of hexagonal 2D layers, as showed in Figure-1.

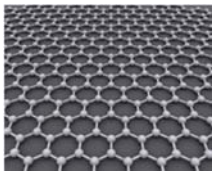

Figure-1. Hexagonal structure of graphene.

In recent years, graphene sheets have been incorporated into a wide array of polymeric matrix, including epoxy, polystyrene, polypropylene and nylon for various functional applications in different industries [9-12]. Numerous previous researches have demonstrated that polymers filled with low graphene loading, i.e. less than 6% significantly enhanced the mechanical, thermal and gas barrier properties of the composites [13-15]. In addition, the flame retardancy character of graphene is also proven to surpasses both montmorillonite and carbon nanotubes with the same filler content [16]. The 2D structure of graphene with its C-C atoms arranged in a hexagonal pattern produces nanoscale gaps that are expected to slow down the release of volatile flammable gases and the layered graphene formed compact char acts as a physical barrier to protect the underlying materials from further burning.

In the current work, two types of graphene, a lab scale experimentally purified expandable graphite and a commercially available graphene were introduced into palm empty fruit bunch (EFB) fiber reinforced epoxy composite. The effects of graphene loading on

morphology, thermal, mechanical and combustibility properties of the composite were investigated.

MATERIALS AND METHODS

Materials

Pulverized oil palm EFB fibers with average bundle diameter in the range of 100-200 μm and 10mm in length were purchased from Szetech Engineering Sdn. Bhd., Malaysia. The matrix system, an ambient cure two part epoxy resin Ultimeg U2020 were purchased from AEV Asia Sdn. Bhd. The epoxy/hardener mixture has a specific viscosity of 1.1 and its viscosity at 25°C was measured 0.2-0.6 Pa·s. The water based formaldehyde-free crosslinked acrylate binding agent Acrodur DS 3530 was supplied by BASF (M) Sdn. Bhd. The water based commercial graphene (CG) nanoplatelets UG PRO 680, with particle size ranging from 1-4 μm was obtained from Ugent Tech (M) Sdn. Bhd. Preparation was performed by drying the CG overnight within a convection oven at 100°C for moisture removal. The lab purified graphene was derived from GRAFGUARD 220-50 grade expandable graphite (EG) flakes manufactured by GrafTech International Ltd., OH, USA. The EG flakes have a typical mean particle size of 350 μm and expansion volume of 200 cm^3/g at 600°C.

Synthetization of Graphene

The expandable graphite (EG) flake was first expanded for a period of 30s within a box furnace preheated to 1000°C to produce expanded graphite oxide (EGO). The enlarged and loosely joined EGO was allowed to cool. An approximately 0.2g of EGO was then placed in a Coors™ high alumina combustion boat of 20ml capacity and inserted into a cylindrical tube. The tube was heated in a ceramic tube furnace maintained at 1000°C for 8h under nitrogen atmosphere to undergo purification.

Preparation of fiber mats

Palm EFB fibers weighting 20g were placed into a customized sieve of dimension 320mm × 180mm (length × width) and subsequently soaked in a mixture of water and Arcodur binder at a ratio of 9:1. The sieve was gently moved in a rounded motion to ensure homogenous fibers distribution across the projected area of the sieve while the suspension was continuously stirred to enhance dispersion of the binding agents. The sieve along with the wet fiber mat were taken out from the water-binder dispersion and left for few minutes to drain out the excess water. Blotting papers followed by metal plates were placed on top and bottom surfaces of the fiber mat. A top load weight of 10kg was placed on the upper metal plate to press out the remaining water. Fully soaked blotting papers were replaced and the pressing process repeated until the fiber mat is dried. The dried fiber mats were then placed in an oven maintained at 70°C for 24h to eliminate the residual moisture.

Fabrication of Nanocomposites

The epoxy palm EFB fiber nanocomposites were prepared by mechanical mixing, ultrasonic dispersing and vacuum resin infusion techniques. The composition for each of the constituent is given in Table-1.

Table-1. Composition of constituent materials.

Sample name	Epoxy (wt%)	EFB (wt%)	Graphene (wt%)
G0	82	18	0
PG001	81.99	18	0.01 (P)
PG002	81.98	18	0.02 (P)
PG003	81.97	18	0.03 (P)
PG004	81.96	18	0.04 (P)
PG005	81.95	18	0.05 (P)
CG005	81.95	18	0.05 (C)

* P = purified graphene ; C = commercial graphene

A predetermined amount of graphene ranging from 0.01-0.05*wt%* was added to the base epoxy resin and the mixture was subjected to high shear within a mechanical mixer maintained at 1000rpm for 1h at ambient temperature. In order to achieve an enhanced deagglomeration and dispersion of graphene, the mixture was exposed to powerful ultrasonication for 1h with the aid of Hielscher UP400S ultrasonic processor, operating at 20Hz and the amplitude was tuned to 100%. Stoichiometric amount of hardener (20 parts hardener to 100 parts base epoxy resin by mass as recommended by the manufacturer) was added to the sonicated volume while gentle stirring was applied to yield a homogenous mixture. The mixture was left to de-gas for 10 min to remove entrapped air bubble prior to infusion.

The dried fiber mat was placed on top of a custom-built mold. A cut to dimension peel ply and infusion mesh were aligned on top of the fiber mat. The setup was entirely covered with a vacuum bagging film and sealed with sealant tape around the exterior perimeter of the mold. The infusion process was initiated with an air removal step, where vacuum applied to the system under the condition that the resin inlet tube was clamped. When hard vacuum (-30 Hg) has been achieved, all connector tubing were clamped and the setup was left under vacuum to check if there is any leakage. Once the system is proved leakage-free, the catalyzed epoxy graphene mixture was infused into the mold to wet the dried fiber mat and subsequently left to cure for 24h at ambient temperature. The cured nanocomposites were removed from mold and

cut into smaller specimens for mechanical, thermal and combustion analyses.

Characterization of mechanical properties

The tensile and flexural properties of the nanocomposites were tested with the aid of a bench type tensile machine Lloyd Instruments LR50K Plus. All tensile experiments were conducted in accordance to the ASTM D3039/3039M standard. Tensile specimens measuring 120mm × 20mm × 2mm (length × width × thickness) were subjected to a constant crosshead speed of 2 mm/min and the resulting force-displacement data were recorded for computation of the nominal stress-strain behaviors. The flexural behavior was measured in a three point bending setup in accordance to ASTM D790 standard. Samples having dimensions of 100mm × 20mm × 2mm (length × width × thickness) were subjected to a crosshead speed of 5 mm/min over a span length of 60mm. Three samples from each material composition were tested and the average value of the respective property was analyzed.

Characterization of thermal properties

The thermal stability of the nanocomposites was characterized using Mettler-Toledo TGA/DSC 1 instrument. Each sample measuring 10 - 15 mg in weight was prepared and placed in an open alumina crucible. The sample was heated from room temperature to 600°C at a constant ramping rate of 20°C/min under nitrogen environment supplied at a flowrate of 50 ml/min. The samples were run in triplicate. The thermal degradation curve with *wt%* loss plot against temperature variation were captured and analyzed.

Characterization of morphological properties

The specimen surface topography was analyzed with FEI Quanta 400F Field Emission Scanning Electron Microscopy (FESEM). The samples were fractured into tiny pieces and surface of interest was mounted upright on a mounting tape prior to scanning under accelerating voltage of 20kV and high vacuum mode.

Characterization of combustibility properties

The nanocomposite specimen gross heat of combustion (GHC) was measured in accordance to ASTM E1740 with the aid of Bomb calorimeter PARR 6100. Specimen fragment weighted less than 1g was placed in a sample cup and the fuse wire was positioned such that it touches the top surface of the solid specimen fragment for combustion to occur.

RESULTS AND DISCUSSIONS

Morphology of PG and CG

SEM micrographs of the PG and CG are showed in Figure-2. It can be seen that PG possesses a worm-like structure typical of expanded graphite, Figure-2(A). When the intercalated graphite is exposed to intent heat within the furnace, the stack of graphite layer planes are forced apart and expanded more than hundred times of its original thickness, resulting in a low density, long and twisted worm-like segment. Magnification to a higher resolution, i.e. at 50μm as showed in Figure-2(B) revealed the exfoliated graphene sheets. The water based CG on the other hand took up a more irregularly shaped powder form, Figure-2(C) and the existence of ~20% moisture causes them to be bonded together, Figure-2(D). Hence proper drying must be conducted prior to the incorporation of the CG into polymer matrix.

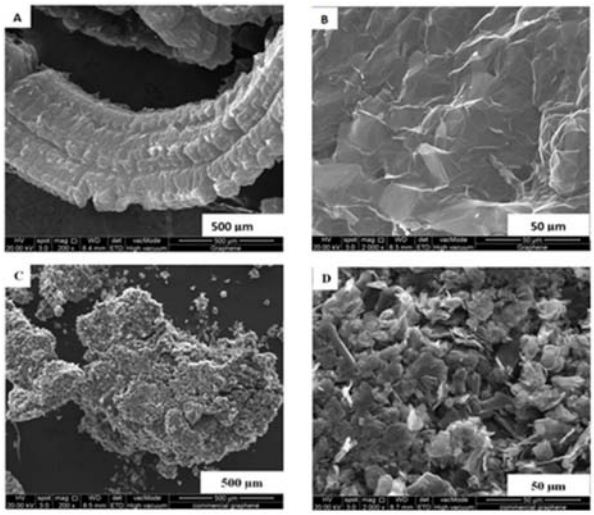

Figure-2. SEM of PG (A), (B) and CG (C), (D).

Mechanical properties

The mechanical properties of the nanocomposites are shown in Figures-3 and Figure-4. It can be observed from Figure-3 that higher tensile and flexural strength were recorded in specimens loaded with a low content of PG, i.e. at 0.01*wt*%. Further increases in the PG loading resulted in the drop of these mechanical properties, potentially due its poor compatibility and agglomeration within epoxy matrix which gives rise to the weak interaction. In general, additives used in high concentrations lead to the reduction in mechanical properties of the polymer matrix [17-18]. Specimen with 0.05*wt*% of PG showed much lower tensile and flexural strength compared to the unfilled epoxy EFB composite, i.e. 0*wt*% PG. This reduction is mainly due to the decreased surface area for fiber–matrix adhesion as a

consequence of the high PG content leading to agglomeration. The interfacial adhesion between reinforcing fiber and polymer matrix also plays an important role on the mechanical properties of the composites [19]. With the same amount of CG graphene loading, i.e. at 0.05*wt*%, specimen with CG demonstrated a more superior mechanical performance compared to those with PG. This could be attributed to the form and surface topography of the CG which allows a better bonding with the epoxy matrix. For the PG, elimination of the oxygen functionalities during purification process at high temperature has adversely affected the interfacial interaction of the system [20].

As depicted in Figure-4, similar response can be observed whereby optimum Young's modulus was found to take place at low PG loading, i.e. at 0.01*wt*% and further increase in PG loading led to a negative impact. Since the reinforcing effect can be realized by graphene loading with a good dispersion, the results suggested that its dispersion in the epoxy matrix was good at low concentration while aggregation tend to takes place and become significant as its content increases [21].

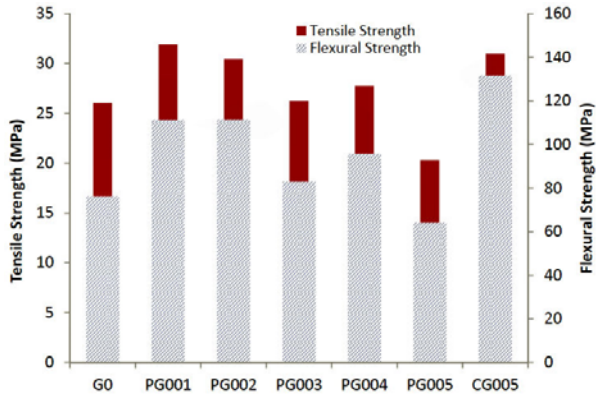

Figure-3. Tensile and flexural strengths of specimens with varying filler compositions.

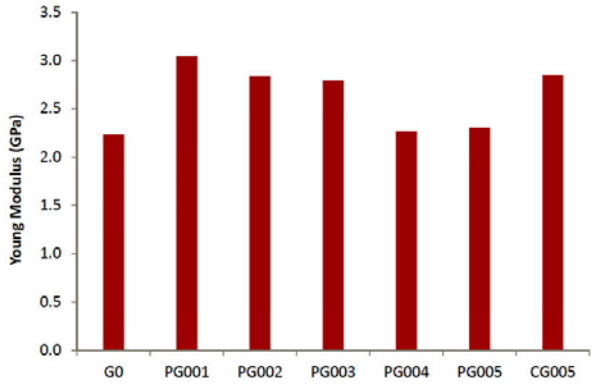

Figure-4. Young's modulus of the specimens.

SEM observations on the fractured surface, showed in Figure-5 indicated that agglomeration becoming more apparent in composition with excessive amount of graphene. At the graphene aggregate sites, i.e. non-exfoliated, micro-sized cracks may initiate and propagated throughout the samples [22]. Therefore, the tensile strength is expected to be lowered by addition of graphene at high concentrations.

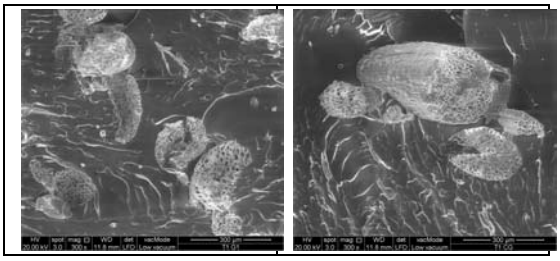

Figure-5. SEM of nanocomposite with 0.01*wt*% (left) and 0.05*wt*% (right) of graphene loadings.

Thermal properties

The use of polymer in high temperature applications often limited by their tendency to degrade at low temperature compared to ceramics or metals. Figure-6 depicts the TGA curves of EFB epoxy composites loaded with various *wt*% of graphene under nitrogen atmosphere.

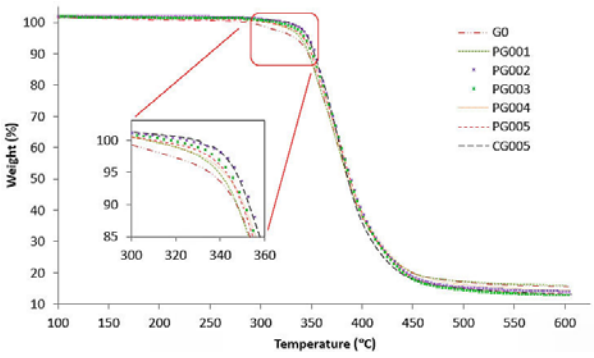

Figure-6. TGA curves of neat epoxy and composites with various *wt*% of graphene.

The degradation temperature corresponding to different percentage weight loss, 5*wt*% (T_{onset}), 50*wt*% (T_{50}) and maximum mass loss rate (T_{max}), i.e. at peak DTG are shown in Table-2.

Table-2. TGA data under nitrogen atmosphere.

Sample name	T_{onset} (°C)	T_{50} (°C)	T_{max} (°C)	Char residue (%) at 600°C
G0	336.33	385.95	373.75	15.56
PG001	339.47	386.03	378.57	15.95
PG002	348.36	389.07	367.77	14.01
PG003	344.54	388.09	382.72	12.85
PG004	341.90	387.29	370.21	14.48
PG005	342.61	388.11	383.40	13.17
CG005	347.12	386.20	380.93	13.02

The initial mass loss below 100°C can be attributed to the evaporation of adsorbed water. The samples were thermally stable up to approximately 300°C where main decomposition took place. In the vicinity of this temperature region, EFB-epoxy composite with 0*wt*% loading of graphene experienced the greatest degradation, with T_{onset} about 3-12°C lower than the rest of the specimen contained graphene fillers. The result indicated that decomposition onset of EFB hemicellulose (220-315°C) and cellulose (315-400°C) within the epoxy composite occurred much earlier in the absent of graphene. Lignin is more thermally stable than cellulosic components and the decomposition of lignin occurred slowly over the whole temperature range owing to its complex aromatic structure with various branches [16, 23-25]. On the other hand, graphene filled nanocomposites showed more superior but relatively similar thermal degradation behavior, which could be attributed to the unique properties of graphene even at low concentration. However, increases in graphene loading do not explicitly resulted in greater thermal stability, whereby T_{50} occurred within 387±2°C. Further degradation occurs with the increase of temperature but gradually settles down between 530-600°C. At 600°C, char residual measuring 12-16 *wt*% remained in the alumina crucible. Wang *et al*. (2014) on their experiments with epoxy melamine phosphate and epoxy 9, 10-Dihydro-9-oxa-10-phosphaphenanthrene-10-oxide observed similar level of char residue at 700°C.

Combustibility properties

The gross heat of combustion (GHC) for the various compositions along with neat epoxy is depicted in Figure-7. Compared to neat epoxy, addition of EFB fibers and graphene reduces the GHC of the composites, i.e. lower heat energy released under complete combustion in the present of oxygen, indicating a poor value fuel source and reduces the likelihood to fire. This could be attributed to the reduction in crosslinking density of the resin matrix whereby a more efficient barrier is formed to impede heat and mass transfer in the combustion event. The results also demonstrated that introducing 0.01 to 0.05*wt*% of graphene (PG or CG) into EFB epoxy composite does not induce any significant effect on the resulting GHC, i.e. the measured GHC remain approximately 31-32 MJ/kg.

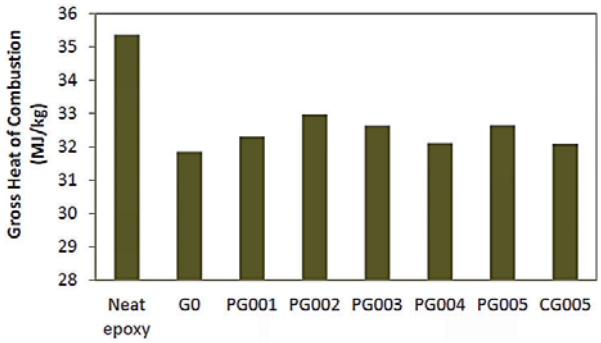

Figure-7. Gross heat of combustion.

Wang *et al*. (2014) reported that the fire retarding mechanism of graphene take place through promotion and formation of compact char layers in condensed phase during the event of combustion within the polymer matrix and the formed char structure effectively separate the matrix from incoming heat and oxygen, hence flaming path being cut off resulted in the reduction in gross heat value.

CONCLUSIONS

Purified graphene prepared through exfoliation of expanded graphite oxide under high heat intensity showed a worm-like structure typical of expanded graphite. Evaluation of EFB epoxy nanocomposites with varying loading of PG and CG in the range of 0.01 to 0.05*wt*% revealed that the mechanical properties improved with low graphene loading. However agglomeration occurred with increasing graphene concentration, leading to the drop in mechanical behaviors of the nanocomposites. In term of thermal stability and combustibility properties, specimens containing EFB fibers and graphene fillers appeared more thermally stable and produced lower GHC compared to neat epoxy. Increasing the graphene concentration from 0.01 to 0.05*wt*% did not impart any significant effect on the resulting thermal and combustion behaviors of the materials. At the same filler loading, CG seem to be slightly more compatible with the resin matrix and ease of dispersion compared to the PG, which could be attributed to its powder form surface topography that facilitate better bonding with the matrix molecules.

ACKNOWLEDGEMENT

This work was supported in part by the Ministry of Science, Technology and Innovation (MOSTI) Malaysia under Grant 03-02-12-SF0212 as well as the Faculty of Engineering at The University of Nottingham Malaysia

Campus. The authors would like to thanks BASF (Malaysia) for supplying the Acrodur water based binder.

REFERENCES

[1] Tshai K.Y., Chai A.B., Kong I., Hoque M.E., Tshai K.H. 2014. Hybrid fibre polylactide acid composite with empty fruit bunch: chopped glass strands, Journal of Composites. 2014(987956): 1-7.

[2] Tshai K.Y., Tan H.J., Khiew P.S., Hoque M.E., Chia C.H. 2015. Effects of aluminum trihydrate on the flame-retardant and smoke-suppressant properties of natural fibres filled composites, Polymers Research Journal. 9(2): 1-15.

[3] Van Den Oever M.J.A., Beck B., Müssig J., 2010. Agrofibre reinforced poly (lactic acid) composites: Effect of moisture on degradation and mechanical properties, Composites Part A. 4(11): 1628-1635.

[4] Demir H., Atikler U., Balköse D., Tıhmınlıoğlu F. 2006. The effect of fiber surface treatments on the tensile and water sorption properties of polypropylene–luffa fiber composites, Composites Part A. 37(3): 447-456.

[5] Choi S., Im H., Kim J., 2012. The thermal conductivity of embedded nano-aluminum nitride-doped multi-walled carbon nanotubes in epoxy composites containing micro-aluminum nitride particles, Nanotechnology. 23(6): 1-10.

[6] Yu A., Ramesh P., Sun X., Bekyarova E., Itkis M.E., Haddon R.C. 2008. Enhanced thermal conductivity in a hybrid graphite nanoplatelet - carbon nanotube filler for epoxy composites, Advanced Materials. 20(24): 4740-4744.

[7] Schwamb T., Burg B.R., Schirmer N.C., Poulikakos D. 2009. An electrical method for the measurement of the thermal and electrical conductivity of reduced graphene oxide nanostructures, Nanotechnology. 20(40): 1-5.

[8] Galpaya D., Wang M., Liu M., Motta N., Waclawik E., Yan C. 2012. Recent advances in fabrication and characterization of graphene-polymer nanocomposites, Graphene. 1(2): 30-49.

[9] Li Y., Pan D., Chen S., Wang Q., Pan G., Wang T. 2012. In situ polymerization and mechanical, thermal properties of polyurethane/graphene oxide/epoxy nanocomposites, Materials and Design. 47: 850-856.

[10] Jiang L., Shen X.P., Wu J.L., Shen K.C. 2010. Preparation and characterization of graphene/poly (vinyl alcohol) nanocomposites. Journal of Applied Polymer Science. 118(1): 275-279.

[11] Kalaitzidou K., Fukushima H., Drzal L.T. 2007. A new compounding method for exfoliated graphite-polypropylene nanocomposites with enhanced flexural properties and lower percolation threshold, Composites Science and Technology. 67(10): 2045-2051.

[12] Jin J., Rafiq R., Gill Y.Q., Song M. 2013. Preparation and characterization of high performance of graphene/nylon nanocomposites, European Polymer Journal. 49(9): 2617-2626.

[13] Rafiee M.A., Rafie J., Wang Z., Song H., Yu Z.Z., Koratkar N. 2009. Enhanced mechanical properties of nanocomposites at low graphene content, American Chemical Society Nano. 3(12): 3884-3890.

[14] Wang S., Tambraparni M., Qiu J., Tipton J., Dean D. 2009. Thermal expansion of graphene composites, Macromolecules. 42: 5251-5255.

[15] Pandele A.M., Ionita M., Crica L., Dinescu S., Costache M., Iovu H. 2014. Synthesis, characterization, and in vitro studies of graphene oxide/chitosan–polyvinyl alcohol films, Carbohydrate Polymers. 102: 813-820.

[16] Huang Y.F., Kuan W.H., Chiueh P.T., Lo S.L. 2011. Pyrolysis of biomass by thermal analysis-mass spectrometry (TA-MS), Bioresource Technology. 102: 3527-3534.

[17] Dai JF, Li B. 2010. Synthesis, thermal degradation, and flame retardance of novel triazine ring-containing macromolecules for intumescent flame retardant polypropylene. Journal of Applied Polymer Science. 116(4): 2157-2165.

[18] Isitman NA, Kaynak C. 2010. Nanoclay and carbon nanotubes as potential synergists of an organophosphorus flame-retardant in poly (methyl methacrylate), Polymer Degradation and Stability. 95(9): 1523-1532.

[19] Wang X., Song L., Pornwannchai W., Hu Y., Kandola B. 2013. The effect of graphene presence in flame retarded epoxy resin matrix on the mechanical and flammability properties of glass fiber-reinforced composites, Composites Part A. 53: 88-96.

[20] Cai D., Song M. 2010. Recent advance in functionalized graphene/polymer nanocomposites, Journal of Materials Chemistry. 20: 7906-7915.

[21] Shen X.J., Liu Y., Xiao H.M., Feng Q.P., Yu Z.Z., Fu S.Y. 2012. The reinforcing effect of graphene nanosheets on the cryogenic mechanical properties of epoxy resins, Composites Science and Technology. 72: 1581-1587.

[22] Yang J.P., Yang G., Xu G., Fu S.Y. 2007. Cryogenic mechanical behaviors of MMT/epoxy nanocomposites, Composites Science and Technology. 67(14): 2934-2940.

[23] Sanchez-Silva L., Lopez-Gonzalez D., Villasenor J., Sanchez P., Valverde J.L. 2012. Thermogravimetric-mass spectrometric analysis of lignocellulosic and marine biomass pyrolysis, Bioresource Technology. 109: 163-172.

[24] Yang H., Yan R., Chen H., Lee D.H., Zheng C. 2007. Characteristics of hemicellulose, cellulose and lignin pyrolysis, Fuel. 86: 1781-1788.

[25] Wang X., Xing W., Feng X., Yu B., Song L., Hu Y. 2014. Functionalization of graphene with grafted polyphosphamide for flame retardant epoxy composites: synthesis, flammability and mechanism, Polymer Chemistry. 5: 1145-1154.